Physics in Medicine & Biology

NOTE

Achieving reliable coincidence resolving time measurement of PET detectors using multichannel waveform digitizer based on DRS4 chip

To cite this article: Haewook Park *et al* 2018 *Phys. Med. Biol.* **63** 24NT02

IOP Publishing Phys. Med. Biol. 63 (2018) 24NT02 (7pp) https://doi.org/10.1088/1361-6560/aaf0bb

Physics in Medicine & Biology

IPEM Institute of Physics and Engineering in Medicine

CrossMark

RECEIVED
12 May 2018

REVISED
22 October 2018

ACCEPTED FOR PUBLICATION
14 November 2018

PUBLISHED
10 December 2018

NOTE

Achieving reliable coincidence resolving time measurement of PET detectors using multichannel waveform digitizer based on DRS4 chip

Haewook Park[1,2], **Seungeun Lee**[1,2], **Guen Bae Ko**[3,4] and **Jae Sung Lee**[1,2,3,4,5]

1 Department of Biomedical Sciences, Seoul National University College of Medicine, Seoul 03080, Republic of Korea
2 Department of Nuclear Medicine, Seoul National University College of Medicine, Seoul 03080, Republic of Korea
3 Institute of Radiation Medicine, Medical Research Center, Seoul National University College of Medicine, Seoul 03080, Republic of Korea
4 Brightonix Imaging Inc., Seoul 03080, Republic of Korea
5 Author to whom any correspondence should be addressed.

E-mail: jaes@snu.ac.kr

Keywords: position emission tomography (PET), timing resolution, coincidence resolving time (CRT), DRS4 chip, multichannel waveform digitizer

Abstract

Coincidence resolving time (CRT) is one of the most important physical-performance measures for positron emission tomography (PET), as reconstruction with accurate time-of-flight information enhances the lesion detectability in patient studies. Accordingly, various PET detector designs and high-performance front-end readout circuits have been actively investigated to improve timing performance. The resulting PET detectors are often evaluated using multichannel waveform digitizers for versatile data analysis of the output signals. However, we have found that inappropriate data acquisition (DAQ) using a multichannel waveform digitizer based on the domino-ring-sampler 4 (DRS4) chip can lead to a considerable error when determining CRT. To address this issue, we performed CRT measurements using a pair of Hamamatsu R9800 photomultiplier tube based PET detectors. Then, considering intra- and inter-chip sampling, we employed four different combinations of input channels into the CAEN DT5742B waveform digitizer and obtained 2D CRT maps according to the leading-edge discriminator threshold for assessing each DAQ scheme. The intra-chip CRT measurement exhibited unusual streak patterns in the 2D CRT map and yielded the artificially-low CRT information in PET detector pairs, whereas the inter-chip CRT measurement provided the reliable estimation of timing resolution. Further, we could prevent the high-frequency signal crosstalk among input channels within the DRS4 chip using the inter-chip CRT measurement. We expect that our findings will also be useful for achieving the reliable CRT measurements when using other single-chip-based multichannel waveform digitizers.

1. Introduction

Recent breakthroughs in tomographic imaging systems have led to the improvement of their physical and clinical performances (Kwon *et al* 2017, Park *et al* 2017b, Sajib *et al* 2018). In particular, accurate timing resolution is an essential characteristic in the modern positron emission tomography (PET) system because precise time-of-flight (TOF) information enhances the signal-to-noise ratio of images and subsequent lesion detectability in patient studies (Moses and Derenzo 2007, Karp *et al* 2008, Conti 2011, El Fakhri *et al* 2011, Surti 2015, Hsu *et al* 2017, Son *et al* 2017). Along with advances in both scintillation crystal and photosensor technologies, in many groups, there have been intense researches on PET detector designs and configurations to improve coincidence resolving time (CRT) (Schaart *et al* 2010, Nemallapudi *et al* 2015, Gundacker *et al* 2016, Kwon *et al* 2016, Schmall *et al* 2016, Brunner and Schaart 2017, Bemeking *et al* 2018). Likewise, the development of front-end electronics based on novel readout techniques and high-performance application-specific integrated circuits (ASICs) also enabled faster temporal responses from PET detectors (Chang *et al* 2016, Di Francesco *et al* 2016, Sacco *et al* 2016, Won *et al* 2016, Ko and Lee 2017, Orita *et al* 2017, Park *et al* 2017a, Shen *et al* 2018). The development and evaluation of high-performance PET detectors designed for TOF applications are often conducted using multichannel waveform digitizers, which allow versatile data analysis using the digitized output signals of the detectors (Ronzhin *et al* 2013, Yeom *et al* 2013a, Schellenberg and Goertzen 2014, Cates *et al* 2015, Kim *et al* 2015).

However, we found that inappropriate combinations of input channels into the waveform digitizer that operates based on several switched capacitor array (SCA) based multichannel sampling chips can lead to a considerable error during CRT measurements. In this technical note, we have addressed somewhat overlooked issues when measuring the timing performance of PET detectors using off-the-shelf multichannel waveform digitizers in terms of data acquisition (DAQ) channel selection. In the CRT measurements, we utilized fast photomultiplier tube (PMT) based PET detectors and a 16-channel waveform digitizer endowed with a domino-ring-sampler 4 (DRS4) chip. The DRS4 chip is the fourth generation in a family of SCA-based digitizer developed in Paul Scherrer Institute (PSI), Switzerland (Ritt 2008). Considering intra- and inter-chip waveform sampling, we here present two-dimensional planar CRT maps (i.e. 2D CRT maps) according to the threshold of the leading-edge discriminator (LED) for four combinations of DAQ channels in the waveform digitizer. These CRT maps would reflect the appropriateness of the DAQ scheme for accurate and precise CRT measurements. In addition, we have investigated the crosstalk characteristics of the DRS4 chip which may further compromise the estimation reliability of timing resolution.

2. Materials and methods

2.1. PET detector setup

We employed two identical PET detectors with sub 200 ps full width at half maximum (FWHM) timing resolution, consisting of an R9800 PMT (Hamamatsu Photonics K.K., Hamamatsu, Japan) and a 0.025 mol% cerium-doped lutetium gadolinium oxyorthosilicate ($Lu_{1.8}Gd_{0.2}SiO_5$(Ce); Oxide Co., Yamanashi, Japan) crystal of $4 \times 4 \times 12\,mm^3$ per detector. The crystals were wrapped with an enhanced spectral reflector (ESR) with thickness of 0.065 mm (3M Company, Maplewood, MN, US) and tightly coupled to the center of the PMT entrance window with BC-630 optical grease (Saint-Gobain S.A., Courbevoie, France), which has a refractive index of 1.465.

2.2. DRS4 chip based multichannel waveform digitizer

The 16-channel waveform digitizer (DT5742B; CAEN S.p.A, Viareggio, Italy) that we used in this study is endowed with DRS4 chips and has a maximum sampling rate of 5-Giga-samples per second at a 12-bit sampling resolution. In particular, the DT5742B waveform digitizer consists of two DRS4 chips, chip 0 to handle DAQ channels Ch0–Ch7 and chip 1 to handle DAQ channels Ch8–Ch15. Fast triggering port TR0 was used for external initialization of the waveform digitizer, as its signal simultaneously enables all the DAQ channels in both chips 0 and 1 (Ritt *et al* 2010). Consequently, if the waveform samples are digitized using the two DRS4 chips, the time offset must be eliminated using the TR0 signal given the unavoidable propagation delay between chips 0 and 1 (CAEN 2017).

2.3. Experimental setup and DAQ

We performed CRT measurements inside a light-shielding box using the experimental setup illustrated in figure 1. A high voltage of 1300 V was supplied to both PMTs through an N470 programmable power supply module (CAEN S.p.A, Viareggio, Italy) under an input dynamic range of the DRS4 chip. We used an MMS06-022 ^{22}Na point source (Eckert & Ziegler AG, Berlin, Germany) with nominal diameter of 0.25 mm and located it close to the center of the entrance window of both PMTs to maximize the trigger rate of the waveform digitizer. Here, we utilized a series of nuclear instrumentation modules for coincidence detection of annihilated gamma photons by the following procedures:

- Each PMT dynode signal was divided into two routes using N625 fan-in/fan-out units (CAEN S.p.A, Viareggio, Italy).
- Then, the duplicated PMT dynode signals were fed into N843 constant fraction discriminator modules (CAEN S.p.A, Viareggio, Italy) to obtain a digital output.
- Finally, the discriminator outputs were fed into a two-input N455 AND module (CAEN S.p.A, Viareggio, Italy) for coincidence detection, whose output was used as external trigger for the waveform digitizer.

To evaluate the DAQ channel selection on CRT measurements, we implemented the four different combinations of DAQ channels as shown in figure 2, namely, combinations 1 (channels Ch0 and Ch1; figure 2(a)) and 2 (channels Ch0 and Ch3; figure 2(b)) only from chip 0 for intra-chip CRT measurements, and combinations 3

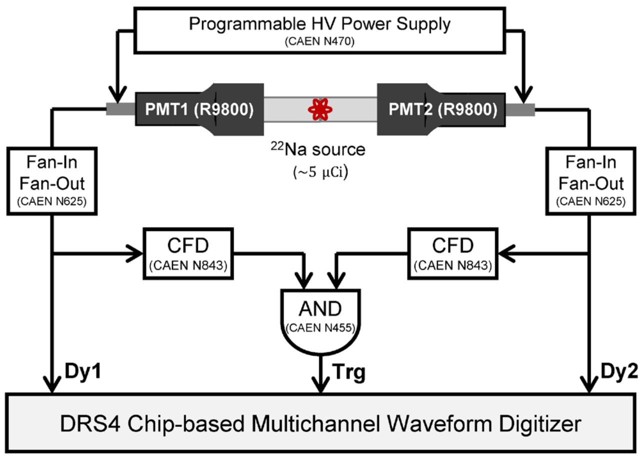

Figure 1. Experimental setup to measure CRT. (HV, high voltage; CFD, constant fraction discriminator; Dy, dynode signal; Trg, trigger signal).

Figure 2. Combinations of input channels for CRT measurements. Intra-chip CRT measurements were performed by selecting DAQ channels from a single DRS4 chip, namely, (a) channels Ch0 and Ch1 and (b) channels Ch0 and Ch3, whereas inter-chip measurements comprised channels from the two different DRS4 chips, namely, (c) channels Ch0 and Ch8 and (d) channels Ch0 and Ch11.

(channels Ch0 and Ch8; figure 2(c)) and 4 (channels Ch0 and Ch11; figure 2(d)) from chips 0 and 1 for inter-chip CRT measurements. The experiments were performed twice using two different DT5742B waveform digitizers to assess the consistency of our findings.

2.4. Data analysis

For the evaluation, we estimated the energy of annihilated gamma photons as the area under the curve during 160 ns. The energy window was set from 410 to 610 keV to reject scattered coincidence events. The arrival time of the photons was derived from the PMT dynode signal by applying a digital LED method with varying thresholds between 10 and 150 mV after baseline correction. The baseline correction was performed by subtracting the mean value of 30 data points before the signal onset of each PMT dynode signal. We have oversampled ($\times$10)

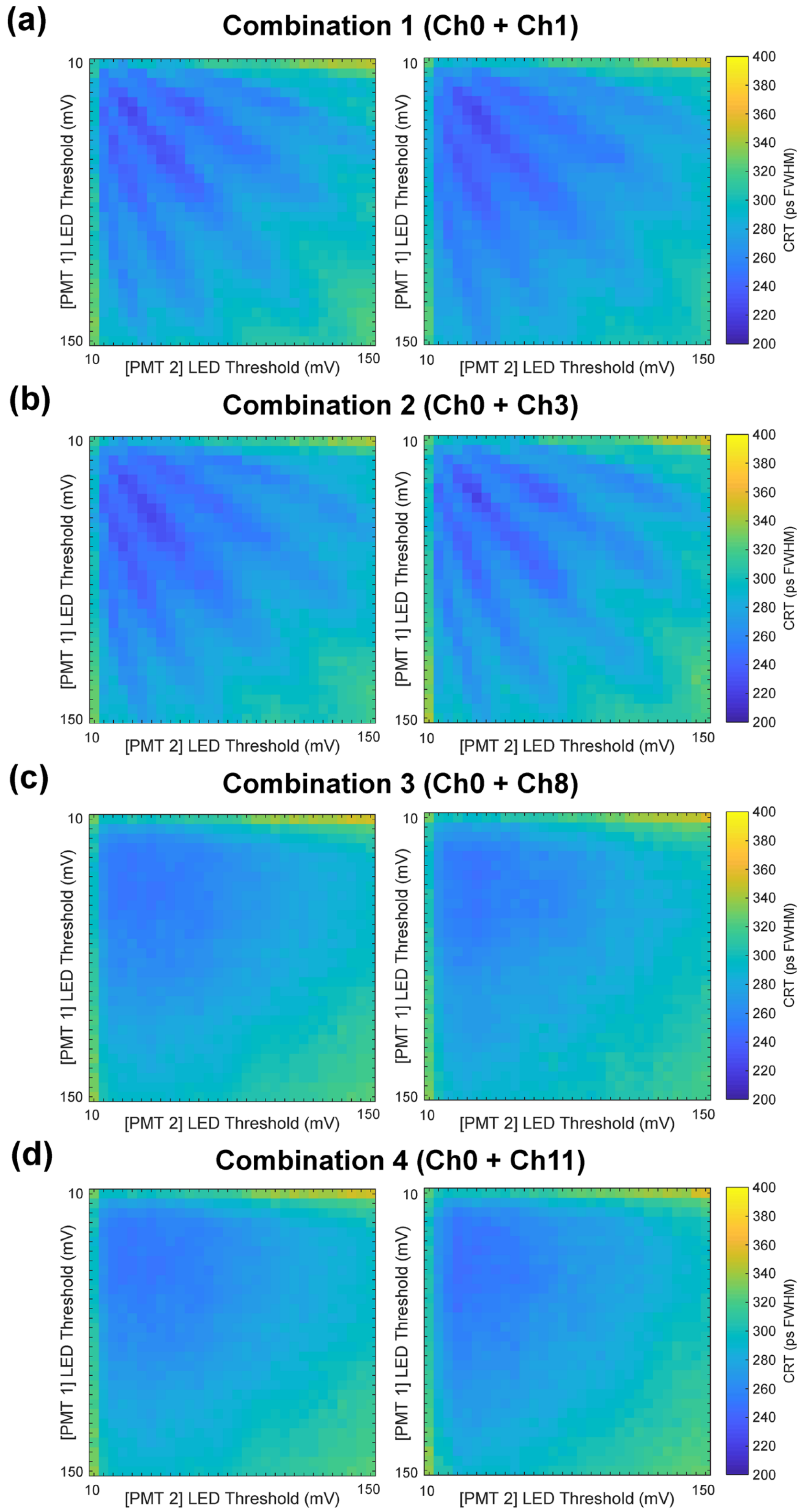

Figure 3. 2D CRT maps according to LED thresholds from two PET detector signals sampled using the combinations of DAQ channels in figure 2: (a) Ch0 and Ch1, (b) Ch0 and Ch3, (c) Ch0 and Ch8, and (d) Ch0 and Ch11.

using cubic spline interpolation to reduce the effect of quantization error. Subsequently, we generated 2D CRT maps according to the LED thresholds to demonstrate the appropriateness of each DAQ scheme.

3. Results and discussions

Single time resolution (STR) of the PET detector measured using LED is a function of the time-pickoff threshold and retrieves a convex shape such as that of figure 6(b) in Lee *et al* (2018) with minimum (i.e. the best STR

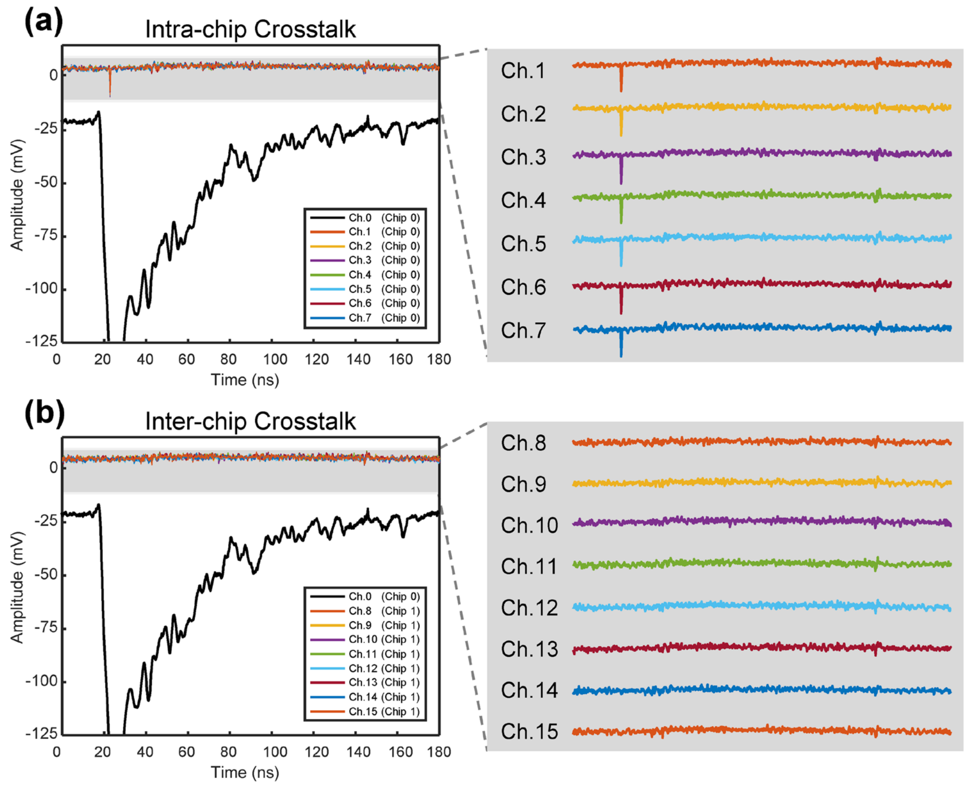

Figure 4. Output signals from DAQ channels of the DT5742B waveform digitizer while feeding a PMT dynode signal to the channel Ch0. (a) Channels Ch1–Ch7 are handled by the single DRS4 chip (chip 0), as well as channel Ch0. (b) Channels Ch8–Ch15 are handled by the other DRS4 chip (chip 1).

value) for some thresholds that depends on both the dark noise level in photosensors at very low thresholds and the increasing time walk at higher thresholds. The CRT of two PET detectors is the quadratic sum of STR of individual detectors as the timing measurements are independent among detectors:

$$\mathrm{CRT}_{\mathrm{Det1/Det2}}(th1, th2) = \sqrt{\mathrm{STR}^2_{\mathrm{Det1}}\,(th1) + \mathrm{STR}^2_{\mathrm{Det2}}\,(th2) + \sigma^2_{\mathrm{noise}}}$$

where $th1$ and $th2$ are the LED thresholds applied to detectors 1 and 2, respectively, and σ_{noise} is the noise contribution from components such as photosensors, scintillators, and readout electronics. Figure 5 in Seifert *et al* (2009) and figure 7 in Yeom *et al* (2013b) show typical 2D CRT maps generated by applying various LED thresholds to two PET detectors and illustrate the independent timing measurement.

In contrast, the 2D CRT maps of intra-chip CRT measurements in figures 3(a) and (b) show streak patterns that might indicate some correlation between the two detectors in either the waveform sampling or timing measurement, whereas the inter-chip measurement results in figures 3(c) and (d) exhibit the normal aspect of 2D CRT maps similar to the aforementioned references (Seifert *et al* 2009, Yeom *et al* 2013b). The results using the two DT5742B waveform digitizers are consistent (i.e. left and right columns in figure 3), thus discarding that the streak patterns in figures 3(a) and (b) are produced by malfunction of the waveform digitizers. The distortion (i.e. streak patterns) in the 2D CRT maps was not related to the physical distance among DAQ channels of the digitizer, as confirmed by the similarity of the distortion between two different combinations of DAQ channels (figures 3(a) and (b)). Although we used the same PET detector pairs in all the experiments, the intra-chip CRT measurement (figures 2(a) and (b)) yielded the artificially-low CRT value of 243 ps FWHM compared to the 263 ps FWHM of the inter-chip CRT measurement (figures 2(c) and (d)). Negligible differences were observed among the outcomes of the two different DT5742B waveform digitizers.

The previous work by Stricker-Shaver *et al* (2014) addressed that an inequidistant sampling interval of the DRS4 chip causes the streak patterns throughout the 2D CRT maps and subsequently deteriorates the reliability of the CRT measurement. To improve the accuracy of CRT measurements, this publication suggests a useful time calibration method that compensates the deviation of the sampling interval over the preset sampling frequency for each and every DAQ channel within the DRS4 chip. This approach is capable of compensating the unequal propagation time between the adjacent SCA cells, thus providing a less-erroneous CRT measurement platform for the PET detectors. However, the precise time calibration is experimentally laborious and should be individually performed from channel to channel because the sampling jitter of each DAQ channel is randomly distributed depending on the CRT measurement setup. Therefore, in the aspect of simplicity, the inter-chip CRT measurement would be the simple but robust alternative for avoiding undesirable sampling error without applying an additional time calibration method.

Figure 12 in the Stricker-Shaver *et al* (2014) indicated that intrinsic sampling jitters from both the single DRS4 chip and the two independent DRS4 chips based measurements were similar to each other, yielding the value of less than 10 ps FWHM for all cable delays. As the typical CRT value from the pair of PET detectors is currently on the order of a few hundred pico-second, the time jitter provoked by the selection of measurement schemes (i.e. intra- and inter-chip measurements) would attribute negligible effect on the timing performance of the PET detectors.

Aside from the 2D CRT maps, we have observed the output signals from all the DAQ channels after feeding a PMT dynode signal only to DAQ channel Ch0 to further investigate the crosstalk characteristics within the DRS4 chip. Figure 4(a) shows the output signals of the seven channels (i.e. Ch1–Ch7) corresponding to the first chip (chip 0) that are clearly affected by crosstalk that aligns with a falling slope of the PMT signal, whereas the other channels (i.e. Ch8–Ch15) corresponding to the second chip (chip 1) do not exhibit a crosstalk artifact, as shown in figure 4(b). In fact, the two DRS4 chips in the DT5742B waveform digitizer simultaneously sample the 16 input signals, and hence it appears that on-chip crosstalk during intra-chip sampling might be another potential cause of erroneous CRT measurements, inducing the baseline fluctuation that behaves like dark noise to the scintillation pulse. We hypothesize that the parasitic capacitance produced among the adjacent DAQ channels within the DRS4 chip would be the underlying reason. Since the signal crosstalk among the DAQ channels is not correlated with the inequidistant sampling nature of the DRS4 chip, therefore the intra-chip measurement may still suffer from the on-chip crosstalk even after the proper time calibration is performed. Further studies would be of high value to investigate the origin of the on-chip signal crosstalk and its aspect to the intra-chip measurement after the time calibration as a future work.

4. Summary and conclusions

In this study, we have explored the overlooked aspects while measuring the timing performance of the PET detector pairs using the 16-channel waveform digitizer endowed with two DRS4 chips. Experimental results have shown that using input channels from the same DRS4 chip (i.e. intra-chip measurement) leads to high-frequency signal crosstalk (figure 4) and distortion in the 2D CRT map (figure 3). Based on the results, we recommend avoiding the intra-chip measurement when evaluating the timing resolution of PET detectors with fast scintillation crystals and photosensors, unless the proper time calibration is performed. Alternatively, we suggest applying the inter-chip CRT measurement which offers the simple but reliable estimation of the timing resolution without the additional time calibration of the DRS4 chip, as well as preventing the undesirable high-frequency crosstalk by adopting DAQ channels from the two different sampling chips. We expect that our findings regarding the DAQ channel influence on CRT measurements using waveform digitizers endowed with DRS4 chips can be applied to obtain reliable CRT information when using other types of single-chip-based multichannel waveform digitizers.

Acknowledgments

This work was supported by grants from National Research Foundation of Korea (NRF) funded by Korean Ministry of Science, ICT and Future Planning (grant nos. NRF-2014M3C7034000 and NRF-2016R1A2B3014645), and Korea Health Technology R&D Project through Korea Health Industry Development Institute (KHIDI), funded by Ministry of Health & Welfare, Republic of Korea (grant no. HI14C1135). We thank Hiroyuki Ishibashi and Yasunori Furukawa (Oxide Co.) for providing us fast LGSO crystal samples.

ORCID iDs

Jae Sung Lee https://orcid.org/0000-0001-7623-053X

References

Bemeking A, Gola A, Ferri A, Finster F, Rucatti D, Paternoster G, Shan N J, Piemonte C and Lerche C 2018 A new PET detector concept for compact preclinical high-resolution hybrid MR-PET *Nucl. Instrum. Methods Phys. Res.* A **888** 44–52

Brunner S E and Schaart D R 2017 BGO as a hybrid scintillator/Cherenkov radiator for cost-effective time-of-flight PET *Phys. Med. Biol.* **62** 4421–39

CAEN 2017 UM4270-DT5742 user manual rev. 8 p 25 (https://www.caen.it/?downloadfile=179)

Cates J W, Bieniosek M F and Levin C S 2015 Strategies for achieving <200 ps coincidence timing resolution with highly multiplexed SiPM arrays *IEEE Nuclear Science Symp. Medical Imaging Conf. Record* pp 1–3

Chang C-M, Cates J W and Levin C S 2016 Time-over-threshold for pulse shape discrimination in a time-of-flight phoswich PET detector *Phys. Med. Biol.* **62** 258–71

Conti M 2011 Improving time resolution in time-of-flight PET *Nucl. Instrum. Methods Phys. Res.* A **648** S194–S

Di Francesco A, Bugalho R, Oliveira L, Rivetti A, Rolo M, Silva J C and Varela J 2016 TOFPET2: a high-performance circuit for PET time-of-flight *Nucl. Instrum. Methods Phys. Res.* A **824** 194–5

El Fakhri G, Surti S, TrottC M, Scheuermann J and Karp J S 2011 Improvement in lesion detection with whole-body oncologic time-of-flight PET *J. Nucl. Med.* **52** 347–53

Gundacker S, Acerbi F, Auffray E, Ferri A, Gola A, Nemallapudi M V, Paternoster G, Piemonte C and Lecoq P 2016 State of the art timing in TOF-PET detectors with LUAG, GAGG and L(Y)SO scintillators of various sizes coupled to FBK-SiPMs *J. Instrum.* **11** P08008

Hsu D F C, Ilan E, Peterson W T, Uribe J, Lubberink M and Levin C S 2017 Studies of a next-generation silicon-photomultiplier-based time-of-flight PET/CT system *J. Nucl. Med.* **58** 1511–8

Karp J S, Surti S, Daube-Witherspoon M E and Muehllehner G 2008 Benefit of time-of-flight in PET: experimental and clinical results *J. Nucl. Med.* **49** 462–70

Kim H, Chen C-T, Eclov N, Ronzhin A, Murat P, Ramberg E, Los S, Wyrwicz A M, Li L and Kao C-M 2015 A feasibility study of a PET/MRI insert detector using strip-line and waveform sampling data acquisition *Nucl. Instrum. Methods Phys. Res.* A **784** 557–64

Ko G B and Lee J S 2017 Single transmission-line readout method for silicon photomultiplier based time-of-flight and depth-of-interaction PET *Phys. Med. Biol.* **62** 2194–207

Kwon H W, Becker A-K, Goo J M and Cheon G J 2017 FDG whole-body PET/MRI in oncology: a systematic review *Nucl. Med. Mol. Imaging* **51** 22–31

Kwon S I, Gola A, Ferri A, Piemonte C and Cherry S R 2016 Bismuth germinate coupled to near ultraviolet silicon photomultipliers for time-of-flight PET *Phys. Med. Biol.* **61** L38–47

Lee S, Lee M S, Won J Y and Lee J S 2018 Performance of a new accelerating-electrode-equipped fast-time-response PMT coupled with fast LGSO *Phys. Med. Biol.* **63** 05NT03

Moses W W and Derenzo S E 2007 Recent advances and future advances in time-of-flight PET *Nucl. Instrum. Methods Phys. Res.* A **580** 919–91

Nemallapudi M V, Gundacker S, Lecoq P, Auffray E, Ferri A, Gola A and Piemonte C 2015 Sub-100 ps coincidence time resolution for positron emission tomography with LSO:Ce codoped with Ca *Phys. Med. Biol.* **60** 4635–49

Orita T, Koyama A, Yoshino M, Kamada K, Yoshikawa A, Shimazoe K and Sugawara H 2017 The current mode time-over-threshold ASIC for a MPPC module in a TOF-PET system *Nucl. Instrum. Methods Phys. Res.* A accepted (https://doi.org/10.1016/j.nima.2017.11.097)

Park H, Ko G B and Lee J S 2017a Hybrid charge division multiplexing method for silicon photomultiplier based PET detectors *Phys. Med. Biol.* **62** 4390–405

Park S, Jung U, Lee S, Lee D and Kim C 2017b Contrast-enhanced dual mode imaging: photoacoustic imaging plus more *Biomed. Eng. Lett.* **7** 121–33

Ritt S 2008 Design and performance of the 6 GHz waveform digitizing chip DRS4 *IEEE Nuclear Science Symp. Conf. Record* pp 1512–5

Ritt S, Dinapoli R and Hartmann U 2010 Application of the DRS chip for fast waveform digitizing *Nucl. Instrum. Meth. Phys. Res.* A **623** 486–4

Ronzhin A *et al* 2013 A SiPM-based TOF-PET detector with high speed digital DRS4 readout *Nucl. Instrum. Methods Phys. Res.* A **703** 109–13

Sacco I, Dohle R, Fischer P, Piemonte C and Ritzert M 2016 A compact, high-density gamma-detection module for time-of-flight measurements in PET applications *Nucl. Instrum. Methods Phys. Res.* A **824** 233–6

Sajib S Z K, Kwon O I, Kim H J and Woo E J 2018 Electrodeless conductivity tensor imaging (CTI) using MRI: basic theory and animal experiments *Biomed. Eng. Lett.* **8** 273–82

Schaart D R, Seifert S, Vinke R, Van Dam H T, Dendooven P, Lohner H and Beekman F J 2010 $LaBr_3$:Ce and SiPMs for time-of-flight PET: achieving 100 ps coincidence resolving time *Phys. Med. Biol.* **55** N179–89

Schellenberg G and Goertzen A L 2014 Evaluation of SiPM photodetectors for use in phoswich detectors *IEEE Nuclear Science Symp. Medical Imaging Conf. Record* pp 1–3

Schmall J P, Surti S, Dokhale P, Ferri A, Gola A, Shah K S and Karp J S 2016 Investigating $CeBr_3$ for ultra-fast TOF-PET detector designs *IEEE Nuclear Science Symp. Medical Imaging Conf. Record* pp 1–4

Seifert S, Vinke R, Van Dam H T, Lohner H, Dendooven P, Beekman F J and Schaart D R 2009 Ultra precise timing with SiPM-based TOF PET scintillation detectors *IEEE Nuclear Science Symp. Conf. Record* pp 2329–33

Shen W, Harion T, Chen H, Briggl K, Stankova V, Munwes Y and Schultz-Coulon H-C 2018 A silicon photomultiplier readout ASIC for time-of-flight applications using a time-of-recovery method *IEEE Trans. Nucl. Sci.* **62** 1196–202

Son J-W, Kim K Y, Yoon H S, Won J Y, Ko G B, Lee M S and Lee J S 2017 Proof-of-concept prototype time-of-flight system based on high-quantum efficiency multianode PMTs *Med. Phys.* **10** 5314–24

Stricker-Shaver D, Ritt S and Pichler B J 2014 Novel calibration method for switched capacitor arrays enables time measurements with sub-picosecond resolution *IEEE Trans. Nucl. Sci.* **61** 3607–17

Surti S 2015 Update on time-of-flight imaging *J. Nucl. Med.* **56** 98–105

Won J Y, Ko G B and Lee J S 2016 Delay grid multiplexing: simple time-based multiplexing and readout method for silicon photomultipliers *Phys. Med. Biol.* **61** 7113–35

Yeom J Y, Vinke R and Levin C S 2013a Optimizing timing performance of silicon photomultiplier-based scintillation detectors *Phys. Med. Biol.* **58** 1207–20

Yeom J Y, Vinke R, Spanoudaki V C, Hong K J and Levin C S 2013b Readout electronics and data acquisition of a positron emission tomography time-of-flight detector module with waveform digitizer *IEEE Trans. Nucl. Sci.* **60** 3735–41